

Nature of the Verwey transition in magnetite (Fe_3O_4) to pressures of 16 GPa

Gregory Kh. Rozenberg, Giovanni R. Hearne,* and Moshe P. Pasternak
School of Physics and Astronomy, Tel-Aviv University, 69978 Tel-Aviv, Israel

P. A. Metcalf and J. M. Honig

Department of Chemistry, Purdue University, 1393 Brown Building, West Lafayette, Indiana 47907-1393

(Received 30 May 1995; revised manuscript received 4 October 1995)

The relative conductivity of Fe_3O_4 single crystals very close to ideal stoichiometry has been measured as a function of pressure up to $P=16$ GPa and in the temperature range of 4.2 to 300 K. The pressure dependence of the Verwey transition T_V and the mechanism of conductivity below T_V were the main issues addressed. Three pressure regimes were assigned, based on the different behavior of the temperature derivative (DT) of the conductivity curves through T_V : (1) In the range 0–6 GPa the DT curves show *sharp* minima at T_V consistent with a first-order phase transition. In this range T_V decreases linearly with pressure from 122 to 107.5 K. (2) At $P>6$ GPa the DT minima *broaden* considerably, consistent with a second- or higher-order transition. At $P\approx 6$ GPa T_V changes discontinuously from 107.5 to 100 K and between 6 and 12.5 GPa decreases linearly to 83 K. (3) At $P>12.5$ GPa no DT minima are detected; T_V becomes indiscernible. It was shown that the variation of T_V with rising P is in close analogy to T_V changes with chemical composition (δ, x, y) of $\text{Fe}_{3(1-\delta)}\text{O}_4$, $\text{Fe}_{3-x}\text{Zn}_x\text{O}_4$, and $\text{Fe}_{3-y}\text{Ti}_y\text{O}_4$ as compiled from previous studies. This information is rationalized in terms of phase transitions associated with “Wigner structures.” Changes in the band gap with rising P are discussed. Below 16 GPa and at $30\text{ K}<T<T_V$ the conductivity σ is typical of the *variable-range hopping* (VRH) mechanism [$\sigma=\sigma_0 \exp(T_0/T)^{1/4}$] with T_0 decreasing with increasing pressure. Below 30 K $\sigma(T)$ deviates from the $T^{1/4}$ law at all pressures.

INTRODUCTION

The Verwey transition in magnetite (Fe_3O_4) has been the subject of numerous studies over many years, ever since the initial work by Millar¹ and by Verwey² and co-workers. Many mechanisms have been proposed to account for the experimental data; this includes partial ordering under the influence of Coulomb interactions among electrons which transfer between iron atoms in octahedrally coordinated interstices. This type of ordering is frequently referred to as Wigner glass crystallization. Experimentally, the transition is manifested as a discontinuity in the resistivity ρ at a fixed temperature $T=T_V\approx 121$ K in stoichiometric magnetite.² It is also detected as an anomaly in the heat capacity.^{1,3} Both in very early work and again only much more recently⁴ it was demonstrated that the Verwey temperature T_V in $\text{Fe}_{3(1-\delta)}\text{O}_4$ diminishes with increasing deviations δ from the ideal composition. Moreover, beyond a critical value $\delta>\delta_c$ one encounters a discontinuity in $d\rho/dT$ rather than in ρ . This reflects a changeover from a first-order to a second- or higher-order phase transformation; the arrangement of Fe^{2+} and Fe^{3+} ions is more ordered below T_V than above that temperature. The nature of ordering is still in dispute; the original proposal of alternating divalent and trivalent iron layers in successive basal planes has been largely discredited in favor of more complicated arrangements.⁵ Heat-capacity studies have confirmed that the latent heat of the transition is suddenly lost in the switch from the first-order to a second- or higher-order transition at $\delta_c=0.0039$. T_V diminishes with increasing δ linearly up to a critical composition δ_c ; there is a discontinuous drop at $\delta=\delta_c$ of roughly 8 K, beyond which T_V again falls linearly with rising δ (see Fig. 4). Near $\delta=3\delta_c$

the transition is lost; beyond that point Fe_3O_4 is unstable, one enters the Fe_2O_3 region of the phase diagram. The low-temperature crystal structure remains in doubt: x-ray-diffraction work⁶ is consistent with a structural transition from the spinel to the monoclinic configuration, whereas magnetoelectric studies^{7–9} lead to the conclusion that the low-temperature phase lacks a center of inversion and is in fact triclinic.

In this paper we report detailed investigations of changes in the Verwey transition when the sample is subjected to quasihydrostatic pressure. This avoids the problem engendered by the disorder generated in the cation sublattice in nonstoichiometric magnetite or when Zn^{2+} or Ti^{4+} is introduced to achieve variations in T_V . High-pressure studies have previously been reported by several authors, but only in the range below 6 GPa and for temperatures between 77 and 300 K. All authors^{10–14} report that T_V drops linearly with increasing pressure P ; however, the reported slope fell into two categories, namely $dT_V/dP=-2.4$ to -2.7 K/GPa or -4.2 to -4.8 K/GPa. This may reflect the difficulties of achieving quasihydrostatic conditions, the taking of measurements without allowing sufficient time for relaxation, and/or the use by some workers of samples of uncontrolled stoichiometry. In the present publication the range of applied pressure and of the temperature region has been greatly extended. Great care has been taken to work with samples of uniform and essentially stoichiometric Fe_3O_4 .

EXPERIMENT

Resistance vs pressure studies have been performed on crystals of pure (99.999%) $\text{Fe}_{3(1-\delta)}\text{O}_4$ ($\delta=0.0006$; $T_V=122$

K) grown by the skull-melter technique,¹⁵ annealed at 1450 °C with annealing time varying from 0.5 to 24 h for samples with thicknesses range from 0.5 to 5 mm. They were subsequently annealed at 1200 °C in a CO/CO₂ atmosphere at a pressure of $\log_{10} P_{\text{O}_2}(\text{atm}) = -6.64$. Details of the sample preparation have been provided elsewhere.¹⁶ For application of pressure a miniature Merrill-Bassett-type diamond-anvil cell¹⁷ was used with culet flat tip diameters of $\sim 500 \mu\text{m}$. A $\sim 200\text{-}\mu\text{m}$ -diam hole, drilled in Ta₉₀W₁₀ gasket preindented to a thickness of 45 μm , served as the sample cavity. The surrounding area was coated with epoxy and with an insulating mixture of Al₂O₃ and NaCl for the resistance vs pressure studies. Some CaSO₄ was prepressed into the cavity to help ensure a quasihydrostatic environment at pressure.¹⁸ A fragment of the original crystal of magnetite was ground and a crystalline of dimensions 150×150×150 μm was loaded onto the CaSO₄ powder at the center of the gasket hole.

Contacts were fabricated onto the culet flat and pavilion facets of one of the anvils to permit four-probe resistance measurements. A thin layer of molybdenum carbide covered with gold film was used as a contact. Formation of the carbide layer was activated by annealing of the Mo covering on the diamond substrate.¹⁹ A mechanical mask placed over the tip of the diamond was used to fabricate four leads on the culet. The average distance between the contact regions which overlap the area of the pressurized sample was $\sim 50 \mu\text{m}$.

Small ruby chips were loaded into the cavity to measure the pressure distribution using the ruby R_1 fluorescence line shift as an indicator. The pressure distribution in the cavity was typically 10–20 % of the average recorded pressure however the pressure gradient in the regions between contacts overlapping the sample area during resistance studies was typically 5–10 %. Pressure variation from 300 to 77 K has been previously²⁰ tested by cooling the miniature cell to 77 K and was found to be at most ~ 1 GPa in the 1–30 GPa range, within the experimental pressure uncertainty. A dipstick arrangement incorporating a miniature Si-diode temperature sensor in close proximity to the anvils was used in a liquid-helium storage Dewar to record the temperature dependence of the resistance $R(T)$ of the pressurized sample. Four-probe dc resistivities were measured between 4.2 and 300 K on both cooling and heating. To increase the accuracy to which the transition temperature could be determined ($140 \geq T \geq 70$ K) thus avoiding thermal lag the cooling and heating rate was ~ 0.3 K/min and with a measurement interval of 0.1 K.

RESULTS

The conductivity (σ) variations with temperature (T) in arbitrary units were first plotted as $\ln \sigma$ vs T^{-1} and then as $\ln(\sigma T)$ vs T^{-1} (Ref. 21). In conformity with previous observations⁴ no significant straight-line region was observed in these graphs. We show in Fig. 1(a) plots of $\ln \sigma$ vs $T^{-1/4}$ (Refs. 22 and 23), these being indicative of variable range hopping.^{24,25} The conductivity plots cover the pressure range 0–16 GPa. Their general behavior, both above and below the transition temperature, is similar at all pressures. The main features of the electrical conductivity variation as a function of pressure are the following:

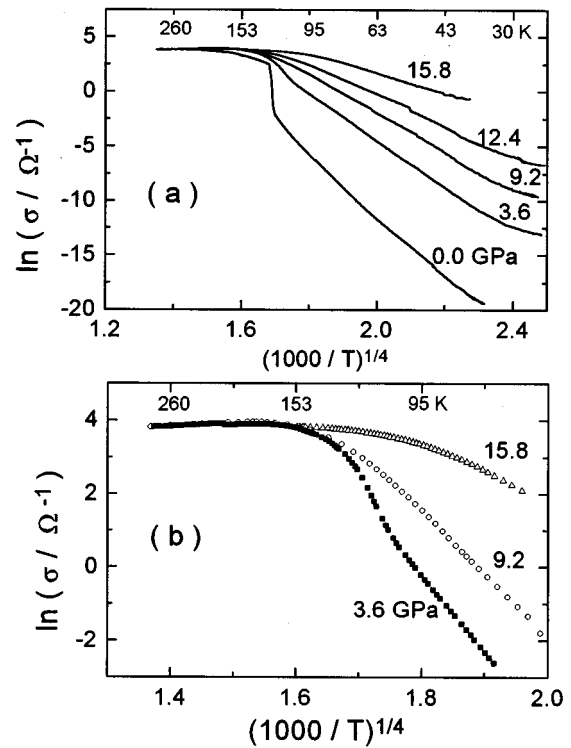


FIG. 1. Temperature dependence of the conductivity, in arbitrary units, of magnetite under pressure. Temperature range (a) 25–300 K, (b) 65–300 K. The data for different samples are normalized to room temperature.

At temperatures $T > T_V$ the conductivity tends to rise slightly with increasing pressure. The same observation was reported in prior work^{10–13} over the pressure range 0–6 GPa. This is intuitively reasonable: The interatomic distances decrease with increasing pressure, thereby raising the conductivity. By contrast, three different effects were noted when pressure was applied to samples for $T < T_V$.

(1) Experiments on a massive sample at ambient pressure indicate a sharp drop in the conductivity as the temperature falls below $T_V = 122$ K; see Fig. 1(a). These results are in conformity with earlier work^{2,4} for strictly stoichiometric samples and are characteristic of a first-order transition. For pressure up to 6 GPa the $\sigma(T)$ plots exhibit distinct changes in slope at the beginning of the transition; the results are displayed in Fig. 1(a); in Fig. 1(b) is shown a more detailed, normalized plot over the range 65–300 K. Because of unavoidable pressure gradients in the cell the transition width is broader at high pressure than under ambient conditions. In this circumstance T_V may be located more accurately by examining the derivative $D = d(\ln \sigma) / d(1/T^{1/4})$. The transition temperature T_V is detected by the pronounced minimum in a plot of D vs $1/T^{1/4}$; representative data are shown in Fig. 2. Very similar T_V values were obtained from plots of $\ln \sigma$ vs $1/T$ and by visual inspection of the midpoint in the temperature range over which the transition is observed.

(2) On increasing the pressure beyond 6 GPa the Verwey transition changes significantly in that it becomes quite diffuse and can be detected only by examining the D vs $1/T^{1/4}$ plots in Fig. 2.

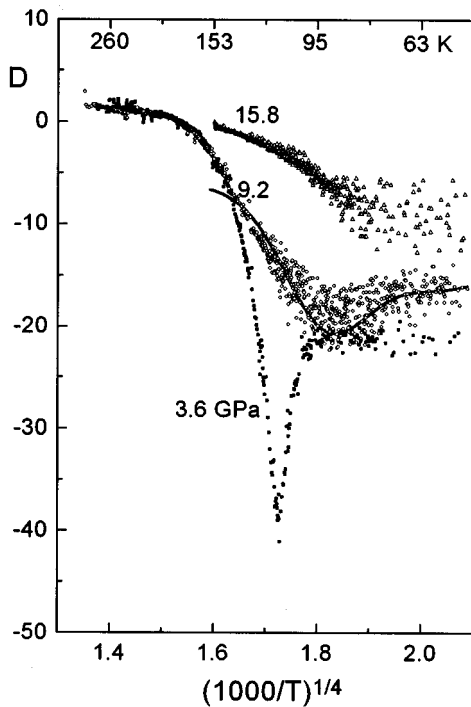


FIG. 2. Typical temperature dependences of the derivative $D = d(\ln\sigma)/d(1/T^{1/4})$ in the first (3.6 GPa) and second order (9.2 GPa) pressure regimes. The solid line represents a Gaussian fitting to the data.

(3) Beyond 12.5 GPa no unusual features are seen in the derivative plot. This indicates that the transition is completely eliminated at pressures $P > 12.5$ GPa.

The above results are summarized in Fig. 3(a) as a plot of T_V vs applied pressure P . This graph bears a remarkable resemblance to the variations in T_V encountered by increasing δ in $\text{Fe}_{3(1-\delta)}\text{O}_4$ or by lightly doping the magnetite with Ti to form $\text{Fe}_{3-y}\text{Ti}_y\text{O}_4$ or with Zn to form $\text{Fe}_{3-x}\text{Zn}_x\text{O}_4$.²⁶ The corresponding composite graph is shown in Fig. 3(b).

In Fig. 3(a) one clearly discerns two regions: the first spans the temperature range 122–107 K in which T_V decreases linearly with rising pressure. The data by Kakudate *et al.*, obtained at pressure below 2 GPa,¹¹ are in excellent

agreement with our own observations. However, the slope reported here is numerically much smaller than that quoted by other workers.^{10,12,13} Such discrepancies can arise if substantial pressure gradients are allowed to be established and/or if the time allotted for all relaxation processes to take effect is insufficient. As has been established by earlier work on magnetite under ambient conditions²⁶ [see also Fig. 3(b)] this region corresponds to the range of first-order transitions; the slope of the line in Fig. 3(a) is -2.5 K/GPa. At the critical value $P = P_c = 6.0$ GPa there is a discontinuous shift to the temperature range 100–82 K, in which T_V again drops with rising pressure. Earlier experiments under ambient conditions²⁵ indicate that this region falls in the regime of a second- or higher-order transition; the slope of the corresponding straight line is -2.9 K/GPa.

At a fixed pressure and from temperatures T_V down to 30 K the conductivity data fairly accurately obey the relation $\ln\sigma = \ln\sigma_0 - (T_0/T)^{1/4}$; typical data are shown in Fig. 4 for magnetite at a pressure of 12.4 GPa. With increasing applied pressure the conductivity increases markedly, and the slope of the straight line diminishes. The data are clearly consistent with the Mott *variable-range hopping* law; T_0 values extracted from those data at various pressure are shown in Table I; $k_B T_0$ range from 3.4×10^4 eV at ambient pressure to 600 eV for $P = 15.8$ GPa (k_B is Boltzmann's constant). The above stands in contrast to the effects of fluorine doping, where T_0 does not change significantly with alterations in F content,²² and is supposed to be the result of band broadening and electron delocalization by decreasing interatomic distances. Deviation from the $T^{1/4}$ power law are encountered for all runs at $T < 30$ K.

DISCUSSION

We compare our experimental results with recent electrical transport measurements on magnetite samples with variable oxygen stoichiometry,⁴ or on crystals lightly doped with titanium,^{26,27} zinc,²⁸ or fluorine.²² In all cases the character of the transition changes very much in the same manner as in the present study; this is documented by comparison of Figs. 3(a) and 3(b). We observed that the two temperature ranges $121 > T_V > 108$ and $101 > T_V > 82$ K for the first- and second-

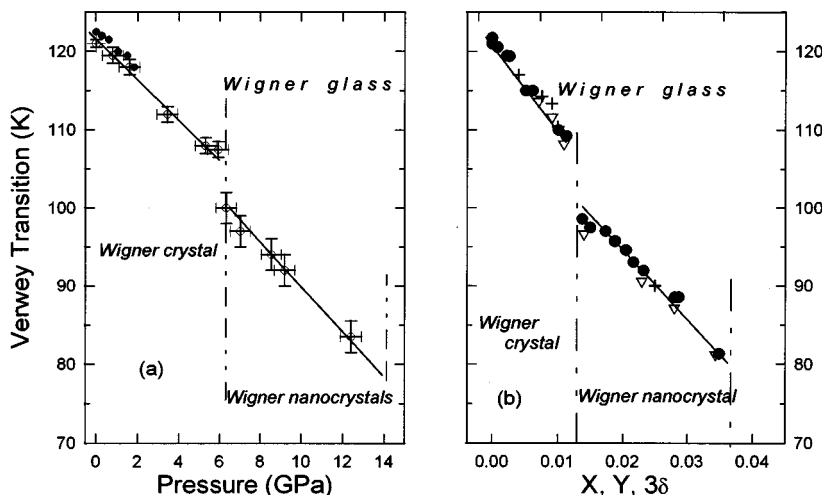


FIG. 3. (a) Pressure variation of T_V and proposed pressure/temperature phase diagram for the structural state of the electron gas in magnetite. ● corresponds to the data of Kakudate *et al.* and ○ corresponds to the present work. (b) Composition variation of T_V at ambient pressure. ● corresponds to the degree of stoichiometry “ 3δ ” in $\text{Fe}_{3(1-\delta)}\text{O}_4$, ▽ corresponds to composition “ x ” in $\text{Fe}_{3-x}\text{Zn}_x\text{O}_4$, and + to the composition “ y ” in $\text{Fe}_{3-y}\text{Ti}_y\text{O}_4$ (see text).

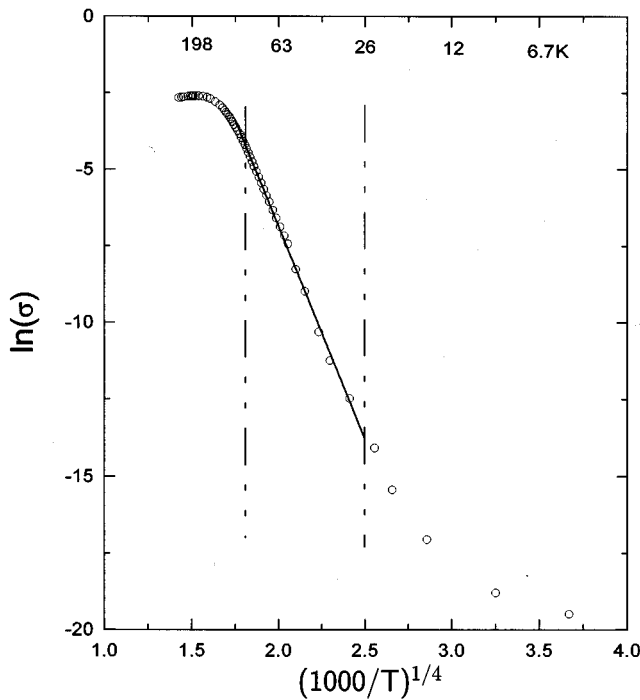


FIG. 4. Typical temperature dependence of the electrical conductivity σ (in arbitrary units) of magnetite at $P=12.4$ GPa in the temperature range 5–300 K. Note the linear relationship of $\ln(\sigma)$ vs $(1000/T^{-1/4})$ in the 30–80 K range.

order regimes are exactly the same, whether the experiments are carried out at ambient pressure via small changes in sample composition or on stoichiometric Fe_3O_4 by altering the pressure. There is nonetheless an important difference: on increasing the pressure dT_V/dP in the second-order regime is greater than in the first-order range. By contrast $dT_V/d\delta$ (or $1/3dT_V/dx=1/3dT_V/dy$ for Zn- or Ti-doped magnetite) is smaller in the second- as compared to the first-order case. The significance of this distinction is presently not understood, but may be related to the fact that the lattice parameter is affected to a much greater degree by the application of pressure than can be achieved by the very small degree of doping required to alter the phase transformation.

The change in the character of the phase transition is detected by differences in various physical properties: the first-order regime is marked by discontinuities in electrical trans-

TABLE I. Pressure variation of the Mott temperature T_0 and the ratio of the localization length α^{-1} to that of the B -site nearest-neighbor distance a .

Pressure (GPa)	$k_B T_0$ (10^4 eV)	$(\alpha a)^{-1}$
0	3.4	0.05–0.11
3.6	1.8	0.063–0.13
5.9	1.0	0.07–0.15
7.0	0.99	0.08–0.16
9.2	0.69	0.09–0.18
12.4	0.25	0.13–0.26
15.8	0.06	0.2–0.43

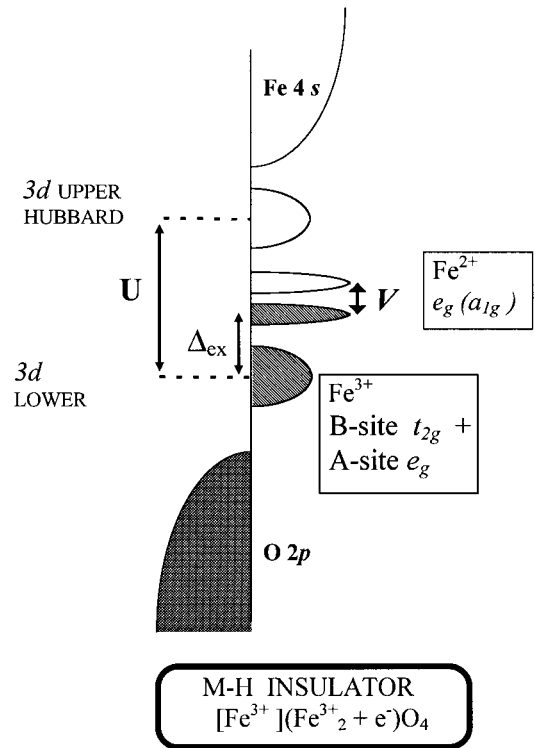


FIG. 5. Energy level scheme proposed for magnetite at ambient pressure and $T < T_V$. Δ_{ex} is the exchange splitting between spin-up and spin-down orbitals on the same cation. Shaded bands are occupied states.

port, entropy, Mössbauer parameters, and the like. In the second-order regime these changes are much more diffuse. For sufficiently high doping levels the transition disappears altogether, and the physical properties similarly change drastically.

The alterations induced by doping all produce quite similar effects and can be correlated with a local loss of charge, electrons through addition of oxygen and zinc, and holes through doping with titanium and fluorine, on octahedrally coordinated iron. However, such a mechanism does not explain the results obtained on application of pressure. We therefore rationalize the coincidence of results by focusing on the on-site repulsion between electrons which are characterized by a Coulomb “gap” $V \sim e^2/ka$, where k is the dielectric constant; a is distance between the nearest-neighbor sites. According to the one-electron picture of magnetite band structure (Fig. 5) (Ref. 29) the additional sixth electron of Fe^{2+} in the B site corresponds to a t_{2g} orbital contribution to the minority-spin band. This band is perturbed by cubic and trigonal components of the crystal field and the extra electron is considered to occupy the lowest-lying (a_{1g}) non-degenerate band. The splitting of the singlet a_{1g} band is then related to the energy V required for a carrier to hop from an Fe^{2+} site to an Fe^{3+} site. Carriers are “frozen” into a charge-ordered state at $T < T_V$ and there is thermal activation across the gap V (~ 40 meV). At $T > T_V$ carrier transport is better ascribed to a *small polaron hopping* mechanism.

Cullen and Callen condition³⁰ have considered only the Coulomb interaction between the “extra” B -site electrons and occupancy of the a_{1g} band in the Hartree approximation

whereas Ihle and Lorenz³¹ have explicitly taken electron correlation effects into account. In either case an ordered insulator will occur for V/B greater than a critical value (for Cullen-Callen condition $V/B=2.2$), where B is the polaron bandwidth. If the system is near the critical condition of V/B a small change of the Coulomb “gap” energy or in bandwidth can bring about a loss of the ordered state, thereby eliminating the Verwey transition. Such a change can be achieved either by diminishing V via a decrease in the average charge per unit cell,³² through doping, or by broadening the polaron band width on application of pressure. This process also increases V via the decrease of a , but this effect is very small [at $P=70$ GPa $\Delta a/a \sim 0.013$ (Ref. 33)].

To understand the observed changes in conductivity at T_V we must consider the electronic state in magnetite under different temperatures and pressures. In earlier treatments of the problem³⁴ considerable emphasis was placed on the strictly short-range, local configurations: using the order-disorder formalism it was possible to rationalize the first- and higher-order transitions within a single mathematical framework. Here we revert to earlier models that to a greater degree emphasize the global ordering aspects. For this purpose we adopt the concept of “Wigner structures.” Mott³⁵ proposed that the electron assembly in magnetite above T_V may be characterized as a “Wigner glass,” electrons are in a localized state generated through interactions with other localized electrons or with impurities or defects. At $T=T_V$ the Wigner glass transforms discontinuously into a “Wigner crystal” at lower T , so long as the electron assembly in the coordinated sites is subject to long range order ($V/B=2.2$). This concept has received considerable support through neutron-scattering experiments:³² in pure Fe_3O_4 additional superlattice reflections set in at the $(h,0,1+1/2)$ positions for temperatures below T_V . This “Wigner crystallization” process is accompanied by the abrupt disappearance of diffuse planar scattering characteristic of short-range order in a Wigner glass above T_V . Planar diffuse scattering was observed over a wide temperature range $T-T_V < 100$ K, which increases rapidly in intensity as the Verwey transition is approached from above. According to our data this type of transition takes place at pressures up to $P=6$ GPa.

With further increase in pressure the correlation length should diminish and the system should result in a low-temperature state characterized exclusively by short-range ordering. In terms of the band picture this is a regime in which V/B is less than the critical value for gap formation ($V/B < 2.2$). In this regime the transition to an ordered state is bypassed and one can assign a Wigner glass state which will cover the entire temperature range. Therefore, no anomalies in the conductivity behavior are expected or encountered such as we observed beyond 12.5 GPa.

To understand the results for the intermediate pressure range we consider recent neutron-scattering experiment on cation-deficient $\text{Fe}_{3(1-\delta)}\text{O}_4$ with $\delta=0.006$,³² in the regime of

the second- or higher-order transitions. Here one no longer encounters long-range order; instead, for $T < T_V$ the material breaks up into domains with finite correlation lengths of approximately 30 unit cells. Diffuse scattering now does not disappear abruptly at T_V but is present as well at lower temperatures. Accordingly, we assume that in the pressure range 6–12.5 GPa Wigner glass below T_V transforms to a new state characterized as a mixture of ordered and disordered regions; the former are characterized by a small correlation length. We refer to these as a “Wigner nanocrystalline state.” In terms of the band picture of Fig. 5 the pressure range 6–12.5 GPa is a regime in which V/B is near to a critical value such that there is incipient gap closure.

From T_0 values we can estimate a localization length α^{-1} using the relation²⁴

$$\alpha^{-1} = [k_B T_0 N(E_F)/16]^{1/3}, \quad (1)$$

where $N(E_F)$ is the density of states at the Fermi level. Expression for the ratio of the localization length to the B -site nearest-neighbor distance a may be derived, namely,

$$(\alpha a)^{-1} \sim 5 [k_B T_0 N^*(E_F)]^{-1/3}, \quad (2)$$

where $N^*(E_F)$ is a normalized density of states. If we assume that $N^*(E_F)$ is in the range of $1-10$ (eV)⁻¹ (Ref. 36) at any given pressure, we are able to calculate a range of values for $(\alpha a)^{-1}$ at each recorded pressure, see Table I. The calculated value 0.05–0.11 of $(\alpha a)^{-1}$ at ambient pressure does not seem to be indicative of a simple variable-range hopping process. This result is not just specific to the present set of measurements; the same T_0 is found for magnetite at ambient pressure in the data of Refs. 22 and 23. At $P=15.8$ GPa $(\alpha a)^{-1} \sim 0.2-0.4$ corresponding to a more significant overlap of the original localized wave functions of the “extra” minority-spin carriers as a result of a decrease in the B -site nearest-neighbor distance under compression. This is consistent with the observed suppression of T_V at this pressure; the extra electrons of the original Fe^{2+} sites are now “shared” between nearest-neighbor B sites at all temperatures.

For $T < 30$ K there are marked deviations from linearity in the plot of Fig. 1. At the lowest temperature the conductivity tends towards a constant value, see Fig. 4. This observation is similar to that reported by Drabble *et al.*²³ and might be linked³⁵ to the idea suggested by Galeszki *et al.*³⁷ of the purported presence of the unstable Fe^+ and Fe^{4+} species in Fe_3O_4 below 20 K.

ACKNOWLEDGMENTS

This work was partially supported by BSF Grant No. 92-0008, ISF Grant No. 451/94, and MSA Grant No. 6326.

*Permanent address: Department of Physics, University of the Witwatersrand, PO Wits 2050, Johannesburg-Gauteng, South Africa.

¹R. W. Millar, *J. Am. Chem. Soc.* **51**, 215 (1929).

²E. J. Verwey and P. W. Haayman, *Physica* **8**, 979 (1941); E. J.

Verwey, P. W. Haayman, and F. C. Romejin, *J. Chem. Phys.* **15**, 181 (1947).

³J. P. Shepherd, J. W. Konitzer, R. Aragon, J. Spalek, and J. M. Honig, *Phys. Rev. B* **43**, 8461 (1991), and references therein.

⁴R. Aragon, R. J. Rasmussen, J. P. Shepherd, J. W. Konitzer, and J.

- M. Honig, *J. Magn. Magn. Mater.* **54-57**, 1335 (1986).
- ⁵M. Mizoguchi, *J. Phys. Soc. Jpn.* **44**, 1572 (1978).
- ⁶M. Iizumi, T. F. Koetzle, G. Shirane, S. Chikazumi, M. Matsui, and S. Todo, *Acta Crystallogr. B* **38**, 2121 (1982).
- ⁷Y. Miyamoto and S. Chikamuzi, *J. Phys. Soc. Jpn.* **57**, 2040 (1988).
- ⁸J. T. Rado and J. M. Ferrari, *Phys. Rev. B* **12**, 5166 (1975).
- ⁹K. Siratori, E. Kita, G. Kaji, A. Tasaki, S. Kimura, I. Shindo, and K. Kohn, *J. Phys. Soc. Jpn.* **47**, 1779 (1977).
- ¹⁰G. A. Samara, *Phys. Rev. Lett.* **21**, 795 (1968).
- ¹¹Y. Kakudate, N. Mori, and Y. Kino, *J. Magn. Magn. Mater.* **12**, 22 (1979).
- ¹²Sheela K. Ramasesha, Murali Mohan, A. K. Singh, J. M. Honig, and C. N. R. Rao, *Phys. Rev. B* **50**, 13 789 (1994).
- ¹³H. H. Schloessin and R. Govindarajan, in *High Pressure in Science and Technology*, edited by C. Homan, R. K. MacCrone, and E. Whalley, MRS Symposia Proceedings No. 22 (Materials Research Society, Pittsburgh, 1984), p. 345.
- ¹⁴S. Tamura, *J. Phys. Soc. Jpn.* **59**, 4462 (1990).
- ¹⁵H. R. Harrison and R. Aragon, *Mater. Res. Bull.* **13**, 1097 (1978).
- ¹⁶R. Aragon, D. J. Buttrey, J. P. Shepherd, and J. M. Honig, *Phys. Rev. B* **31**, 430 (1985).
- ¹⁷A. Jayaraman, *Rev. Mod. Phys.* **55**, 65 (1983).
- ¹⁸Of several transmitting media tested, suitable for electrical conductivity measurements in DAC, the best material found was CaSO₄, see D. Erskine, P. Y. Yu, and G. Martinez, *Rev. Sci. Instrum.* **58**, 406 (1987).
- ¹⁹K. L. Moazed, J. R. Zeidler, and M. J. Taylor, *J. Appl. Phys.* **68**, 2246 (1990).
- ²⁰G. R. Hearne, M. P. Pasternak, and R. D. Taylor, *Rev. Sci. Instrum.* **65**, 3787 (1994). See also R. G. Munro, G. J. Piermarini, S. Block, and W. B. Holzapfel, *J. Appl. Phys.* **57**, 165 (1985).
- ²¹T. E. Whall, K. K. Yeung, Y. G. Proykova, and V. A. Brabers, *Philos. Mag. B* **54**, 505 (1986).
- ²²H. Graener, M. Rosenberg, T. E. Whall, and M. R. Jones, *Philos. Mag. B* **40**, 389 (1979).
- ²³J. R. Drabble, T. D. Whyte, and R. M. Hooper, *Solid State Commun.* **9**, 275 (1971).
- ²⁴J. G. Austin and N. F. Mott, *Adv. Phys.* **18**, 41 (1969).
- ²⁵N. F. Mott, *Metal-Insulator Transitions* (Taylor & Francis, London, 1990).
- ²⁶Z. Kakol, J. Sabol, J. Stickler, and J. M. Honig, *Phys. Rev. B* **46**, 1975 (1992).
- ²⁷A. Kozłowski, R. J. Rasmussen, J. Sabol, P. Metcalf, and J. M. Honig, *Phys. Rev. B* **48**, 2057 (1993).
- ²⁸P. Wang, Z. Kakol, M. Wittenauer, and J. M. Honig, *Phys. Rev. B* **42**, 4553 (1990).
- ²⁹D. L. Camphausen, J. M. Coey, and B. K. Chakraverty, *Phys. Rev. Lett.* **29**, 657 (1972).
- ³⁰J. R. Cullen and E. R. Callen, *Phys. Rev. B* **7**, 397 (1973).
- ³¹D. Ihle and B. Lorenz, *Philos. Mag. B* **42**, 337 (1980).
- ³²R. Aragon, P. M. Gehring, and S. M. Shapiro, *Phys. Rev. Lett.* **70**, 1635 (1993).
- ³³D. R. Wilburn and W. A. Basset, *High Temp. High Pressure* **9**, 35 (1977).
- ³⁴J. M. Honig, *J. Solid State Chem.* **96**, 115 (1992).
- ³⁵N. F. Mott, *Festkörperproblem* **19**, 331 (1979).
- ³⁶V. A. M. Brabers, *Physica B* **205**, 143 (1995).
- ³⁷G. Galeczki and A. A. Hirsch, *J. Magn. Magn. Mater.* **7**, 230 (1978).